Hydrol. Earth Syst. Sci. Discuss., 9, 11487–11520, 2012
www.hydrol-earth-syst-sci-discuss.net/9/11487/2012/
doi:10.5194/hessd-9-11487-2012


Hydrology and Earth System Sciences Discussions



# Analysis of long-term terrestrial water storage variations in Yangtze River basin

**Y. Huang[1,2], M. S. Salama[1], M. S. Krol[2], R. van der Velde[1], A. Y. Hoekstra[2], Y. Zhou[3], and Z. Su[1]**

[1]Faculty of Geo-Information Science and Earth Observation (ITC), Department of Water Resources, University of Twente, Enschede, The Netherlands
[2]Faculty of Engineering Technology, Department of Water Engineering and Management (WEM), University of Twente, Enschede, The Netherlands
[3]State Key Lab of Estuarine and Coastal Research (SKLEC), East China Normal University, Shanghai, China

Received: 28 August 2012 – Accepted: 17 September 2012 – Published: 5 October 2012

Correspondence to: Y. Huang (huang@itc.nl)

Published by Copernicus Publications on behalf of the European Geosciences Union.

## Abstract

In this study, we analyze 32 yr of TWS data obtained from Interim Reanalysis Data (ERA-Interim) and Noah model from Global Land Data Assimilation System (GLDAS-Noah) for the period between 1979 and 2010. The accuracy of these datasets is validated against 26 yr (1979–2004) of runoff dataset from Yichang gauging station and compared to 32 yr of independent precipitation data obtained from Global Precipitation Climatology Centre Full Data Reanalysis Version 6 (GPCC) and NOAA's PRECipitation REConstruction over Land (PREC/L). Spatial and temporal analysis of the TWS data shows that TWS in the Yangtze River basin is decreasing significantly since the year 1998. The driest period of the basin is noted from 2005 to 2010, especially in the middle and lower Yangtze reaches. The TWS changed abruptly into persistently high negative anomalies in the middle and lower Yangtze reaches in 2004. From both basin and annual perspectives, 2006 is detected as the major inflection point at which the system exhibits a persistent decrease in TWS. Comparing these TWS trends to independent precipitation datasets shows that the recent decrease in TWS can mainly be attributed to a decrease in precipitation amount. Our finding is based on observation and modeling data sets and confirms previous results based on gauging station datasets.

## 1 Introduction

Terrestrial water storage (TWS) is defined as all forms of water stored above and underneath the surface of the Earth, including soil moisture, snow and ice, canopy water storage, groundwater etc. As a key component of the terrestrial and global hydrological cycles, TWS exerts important control over the water, energy and biogeochemical fluxes, thereby playing a major role in Earth's climate system (Famiglietti, 2004). TWS is not only an indicator of Earth's climate variability, but also affect various components of Earth's hydrological cycle (Niu and Yang, 2006). Soil moisture plays a key role in





HESSD

9, 11487–11520, 2012

both the water and energy cycle through its impact on the energy partitioning at the surface, and has also links with the biogeochemical cycle via plant transpiration and photosynthesis (Seneviratne et al., 2010). Snow cover has a great influence on the onset of summer monsoon and runoff production in spring (Ding et al., 2009). Therefore, the spatial and temporal variability of TWS under climate change and human induced impacts is an important component that should be taken into account for river basin management.

From a historical perspective, there is limited information about the TWS distribution in time and space, since TWS is not routinely observed like many other hydrometeorological measurements are. Isolated observational datasets are available only for some regions and rarely beyond several years duration. Moreover, in situ observations are point measurements, and are not always representative for large spatial domains (Famiglietti et al., 2008; van der Velde et al., 2008). Fortunately, the progress in satellite remote sensing and corresponding retrieval techniques enables large scale monitoring of land surface states (e.g. soil moisture, temperature), which has the potential of improving our understanding of the spatially heterogeneous hydrometeorological processes. Advances in microwave remote sensing have demonstrated its uses in providing large-scale soil moisture information resulting in satellite missions specifically dedicated to soil moisture (Entekhabi et al., 2010). Microwave observations can, however, only provide information on the top few centimeters of the soil. In addition, Tapley et al. (2004a,b) and others have shown that from sophisticated measurements of the Earth's gravity field the terrestrial water storage change (TWSC) can be inferred on a monthly scale. The first space mission that employs this technology is the Gravity Recovery and Climate Experiment (GRACE) launched at 17 March 2002.

The data assimilation products such as Interim Reanalysis Data (ERA-Interim) and Global Land Data Assimilation System (GLDAS) combine the virtues of in-situ, remote sensing observations and modeling. The models in these systems simulate the main components of TWS and through fusing with other data sources to reduce uncertainties in hydrological interpretations. These systems have been extensively employed for many TWS and related studies, for example, they have been utilized for regional, continental or global TWS variations analysis (Chen et al., 2005; Seneviratne et al., 2004; Syed et al., 2008). Also, these systems offer long record of data which are suitable for long-term analysis, while remote sensing and in-situ observations are most likely time limited.

In this study, we focus on the analysis of the long-term TWS variation in the Yangtze River basin. The Yangtze River, the longest river in China, is one of the world's top ten rivers in terms of water shortage, resulting from intensive human activities in the river basin although it receives a large volume of runoff (Wong et al., 2007). In last three decades, the Yangtze River basin has experienced fundamental changes, e.g. pronounced warming, large population growth, fast economic development, large water consumption and reservoirs construction. The Three Gorges Dam (TGD) is the largest hydroelectric dam and one of the most controversial projects in the world. It has created the largest man-made lake (more than 600 $km^2$ of land) in the world since the dam body was completed in 2006 and the water level reached 156 m at the first time. Such large change in land use will alter many factors such as albedo, regional climate, and hydrological cycle. In recent years, the basin has experienced an increasing trend in the frequency of extreme events, i.e. low runoff in drought years, floods during intense rainfall (Dai et al., 2008; IPCC, 2001). A better understanding of the change in the Yangtze basin and its hydrological state variables is, thus, important. However, previous works were mostly focused on studying the interaction between runoff, precipitation and evapotranspiration in the basin, while little attention has been given to space-time variability of the TWS and its response to climate change and human activates.

Here we examine the spatial and temporal variation of TWS in the Yangtze River basin which will help improving our understanding of the water cycle and the management of the water resources. The specific objectives of this paper are (1) to use ERA-Interim and ERA-Interim dataset to estimate the TWS and TWSC in the period of 1979–2010, (2) to assess the accuracy of TWS from these two datasets in the basin,





HESSD
9, 11487–11520, 2012

(3) to examine the climatology of the spatial pattern of TWS in the basin, (4) to detect the trends and abrupt changes associated with possible causes.

## 2 Study area

The Yangtze River basin lies within the subtropical zone in China. The river originates from the Qinghai-Tibetan Plateau and flows 6300 km eastward to the sea. The upper Yangtze reach, the headwaters, extends from the westernmost point, at Tuotuohe, to Yichang. The middle reach extends from Yichang to Hukou, and the lower reach extends from Hukou to the river mouth near Shanghai. Cuntan, Yichang, Hankou, and Datong are four gauging stations located along the mainstream of the Yangtze (Fig. 1). Cuntan is the entrance of the Three Gorges Dam (TGD), which extends more than 600 km along the mainstream of the Yangtze. The Three Gorges Dam was constructed 37 km upstream from Yichang with multiple purposes: energy generation, flood control and water supply. Hankou is located in the middle reach of the river, and Datong is located at the tidal limit of the river.

## 3 Data sets

### 3.1 ERA-Interim

The ERA-Interim reanalysis dataset contains physically atmosphere and surface analyses covering the period from 1979 to present based on ECMWF'S Integrated Forecast System (IFS) release Cy31r2 (Berrisford et al., 2011; Simmons et al., 2006). The reanalysis incorporates a forecast model with three fully coupled components for the atmosphere, land surface, and ocean waves, and assimilates various types of observations including satellite and ground based measurements. It uses the Tiled ECMWF Scheme for Surface Exchanges over Land (TESSEL, Viterbo and Beljaars, 1995) to simulate the heat and water exchanges between the land and atmosphere.





HESSD
9, 11487–11520, 2012

The TESSEL model structure includes four soil layers (0–7 cm, 7–28 cm, 28–100 cm and 100–289 cm), what type of vegetation scheme and what type of snow scheme. As the latest global atmospheric reanalysis produced by ECMWF, it is evidently confirmed that the performance of the system is substantially improved in certain key aspects (the representation of the hydrological cycle, the quality of the stratospheric circulation, and the consistency in time of the reanalyzed fields) comparing to EAR-40 (Dee et al., 2011).

The monthly means of daily means of volumetric soil water at four layers, snow depth and snow density with spatial resolution of 1.5° during the period of January 1979–December 2010 are used in this study (available at: http://data-portal.ecmwf.int/data/d/interim_moda/).

### 3.2 GLDAS-Noah

The Global Land Data Assimilation System (GLDAS) project supplies users with the model output of "state-of-the-art", land surface schemes forced by atmospheric variables that originate from various data sources. The model has been forced by multiple data sets: bias-corrected ECMWF Reanalysis data in the time period of 1979–1993, biased-corrected National Center for Atmospheric Research (NCAR) Reanalysis data from 1994 to 1999, NOAA/GDAS atmospheric analysis fields in 2000, then a combination of NOAA/GDAS atmospheric analysis fields, spatially and temporally disaggregated NOAA Climate Prediction Center Merged Analysis of Precipitation (CMAP) fields, and observation-based downward shortwave and long wave radiation fields using the method of the Air Force Weather Agency's AGRicultural METeorological modeling system (AGRMET) in the period 2001-present (Rui, 2011).

For this study, we use the model output produced by the Noah land surface scheme. This data is available from 1979 to present at 3-hourly interval. The Noah soil moisture profile includes four layers of 10, 30, 60 and 100 cm from top to bottom, respectively. The monthly products generated through temporal averaging of the 3-hourly products of soil moisture (SM) and snow water equivalent (SWE) during the period of





HESSD
9, 11487–11520, 2012

January 1979–December 2010 are used in this study. Data generated by the GLDAS-Noah is publicly available at: http://ldas.gsfc.nasa.gov/gldas/.

### 3.3 Field data

Monthly river discharge at Yichang Gauging Station (Fig. 1) has been recorded during the period of January 1979 to December 2004. This data set is used to validate ERA-Interim land GLDAS-Noah outputs in the Yangtze River basin.

### 3.4 GPCC

Global Precipitation Climatology Centre (GPCC) offer gauge-based gridded monthly precipitation data sets for the global land surface from 1901 to 2010. The GPCC Full Data Reanalysis Version 6 with spatial resolution of 1.0°, which is fully independent of the precipitation from ERA-Interim and GLDAS-Noah, is used in this study. it uses the complete GPCC station database (ca. 67 200 stations with at least 10 yr of data) available at the time of analysis and is therefore recommended to be used for global and regional water balance studies, calibration/validation of remote sensing based rainfall estimations and verification of numerical models (Schneider et al., 2011).

### 3.5 PREC/L

NOAA's PRECipitation REConstruction over Land (PREC/L), a further gauge-based data set of monthly precipitation over land (Chen, 2002), is included in this study (spatial resolution of 2.5°). PREC/L is based on different collections of gauge data than used for the GPCC, with a large number of stations until 1990s. It has been documented by Wang et al. (2008) having very high anomaly correlation coefficient (root mean square error) with the observation.





HESSD
9, 11487–11520, 2012
Analysis of long-term terrestrial water storage variations
Y. Huang et al.

# 4 Methods

## 4.1 Water storage estimation

TWS is generally defined as all forms of water stored above and underneath the surface of the Earth, namely: soil moisture, canopy water storage, snow water equivalent and ground water, surface water storage, etc. Our analysis of storage is, however, limited to total column soil moisture (TSM) and snow water equivalent (SWE) and cannot give a complete description of the lateral and vertical distribution of water storage until surface and groundwater components are added to land model used here. We also neglect canopy water storage (CWS) which is included in GLDAS-Noah simulation. The reason behind this assumption is that CWS in the Yangtze River basin is very small in comparison to soil moisture (Zhong et al., 2010). Therefore, TWS can be expressed as Eq. (1), where $N$ represents month index.

$$\mathrm{TWS}_N = \mathrm{TSM}_N + \mathrm{SWE}_N \qquad (1)$$

The monthly change in the terrestrial water storage ($\mathrm{TWSC}_N$) can be calculated at each pixel as follows:

$$\mathrm{TWSC}_N = \{\mathrm{TSM}_N + \mathrm{SWE}_N\} - \{\mathrm{TSM}_{N-1} + \mathrm{SWE}_{N-1}\} \qquad (2)$$

This method showed promising results and also compared well with Gravity Recovery and Climate Experiment (GRACE) estimation and the monthly basin-scale terrestrial water balance approach from flux variables (Chen et al., 2009; Rodell et al., 2004; Syed et al., 2008). It is noted that we scaled the ERA-Interim's soil moisture content of the lowermost level to a depth of 1m and summed this value together with the moisture content of the other three layers in order to compare soil moisture products of ERA-Interim to GLDAS-Noah, at the same soil depth.





HESSD
9, 11487–11520, 2012

### 4.2 Statistical analysis

Trend analyses involve linear regression and non-parametric Mann-Kendall (MK) test (Mann, 1945; Kendall, 1975). A linear regression model is used to compute the annual trend of TWS at each pixel. The MK is a rank-based procedure and is applied for detecting the significance of the trends. To analyze the stationarity of the trend in the TWS anomalies, the Mann-Kendall-Sneyers (MKS) test (Sneyers, 1975) is also applied. This test, a sequential version of the MK test, enables not only to detect the significant trends, but also the approximate transition point in the temporal behavior of a series. The forward sequence (UF) and backward sequence (UB) are calculated using the mean and variance of the data. When the points in the forward series are outside the confidence interval, the detection of a significant increasing ($UF > 0$) or a significant decreasing ($UF < 0$) trend is indicated. If an intersection occurs between UF and UB within the confidence interval, then it indicates an inflection (Li et al., 2004, 2007; Moraes et al., 1998).

## 5 Results and discussion

### 5.1 Evaluation and validation

The regional accuracies and reliabilities of ERA-Interim and GLDAS-Noah are assessed by comparing their spatial averaged time series of runoff in the upper Yangtze River generated to observed runoff in the upper Yangtze reach for the period between 1979 and 2004. Figure 2 shows that the ERA-Interim modeled runoff fits the observed values better than GLDAS-Noah in the period between 1979 and 2004. The determination coefficients ($R$-squared) and the root mean square errors (RMSE) between modeled and observed values for ERA-Interim ($R^2_{\mathrm{E-O}}$, $\mathrm{RMSE}_{\mathrm{E-O}}$) and for GLDAS-Noah ($R^2_{\mathrm{G-O}}$, $\mathrm{RMSE}_{\mathrm{G-O}}$) are 0.87 and 4.19, 0.68 and 14.58, respectively. It is noted that the runoff has been consistently underestimated by GLDAS-Noah which is also





HESSD
9, 11487–11520, 2012

confirmed by Zaitchik et al. (2010), and GLDAS-Noah outputs have obvious errors in 1996 and 1997. Apparently, ERA-Interim datasets have higher accuracy and reliability in the Yangtze River basin.

To further explore the quality of these data sets and as precipitation is arguably the most critical input for accurate TWS, precipitation estimates of ERA-Interim and GLDAS-Noah are compared with products of GPCC and PREC/L which are derived more directly from observations. The spatial averaged time series of standardized annual anomalies have been computed and compared between these four data sets. The result is showed in Fig. 3 that there is a notable error in 1996 of GLDAS-Noah and, generally speaking, ERA-Interim precipitation fits PREC/L and GPCC better ($R$-squared between ERA-Interim and PREC/L ($R^2_{\mathrm{E-P}}$), ERA-Interim and GPCC ($R^2_{\mathrm{E-G}}$) is 0.49 and 0.66, respectively) than that of GLDAS-Noah ($R$-squared between GLDAS-Noah and PREC/L ($R^2_{\mathrm{G-P}}$), GLDAS-Noah and GPCC ($R^2_{\mathrm{G-G}}$) is 0.18 and 0.13, respectively). ERA-Interim shows a general good agreement with GPCC and PREC/L, however, there is a clear shift in the latest decade between them, which we will discuss later.

In situ measurements of soil moisture are invaluable for calibrating and validating land surface model and satellite-based soil moisture retrievals. Unfortunately, there is a very low sampling rate (only 1 sample) available in the Yangtze River basin from the International Soil Moisture Network (ISMN) (Dorigo et al., 2011). However, the error structures of ERA-Interim and GLDAS-Noah soil moisture products have been estimated using the triple collocation technique (Dorigo et al., 2010; Scipal et al., 2008). The data qualities of these soil moisture products in the Yangtze River basin can be inferred after comparing the errors of soil moisture estimates in the Yangtze River basin to other locations where have been already validated by in situ measurements. ERA-Interim reanalysis soil moisture is characterized by a relatively low error (mean global error is 0.018 $\mathrm{m^3\,m^{-3}}$) (Dorigo et al., 2010) which is fairly consistent with the average error (mean global error is 0.020 $\mathrm{m^3\,m^{-3}}$) obtained by Scipal et al. (2008) by applying triple collocation model to three satellite-based and model-based soil moisture products, and the Yangtze River basin has relatively low error (close to the global average).

This fact can also be confirmed by the high correlation with ASCAT retrievals for the years 2007 and 2008 (Dorigo et al., 2010) and ERS-2 retrievals for the years 1998, 1999 and 2000 (Scipal et al., 2008). In addition, Liu et al. (2011) showed that there is a high correlation coefficient ($R$) between GLDAS-Noah and ASCAT retrievals in the Yangtze River basin in 2007. It has been expected and firmly proved that active microwave satellite-based (e.g. ASCAT) retrievals provide lower errors in moderately to densely vegetated areas (e.g. the Yangtze River basin) than passive microwave products (Liu et al., 2011). Therefore, the high correlations between ERA-Interim or GLDAS-Noah and active microwave satellite-based soil moisture retrievals somehow provide the confidence in EAR-Interim and GLDAS-Noah soil moisture qualities in the Yangtze River basin.

## 5.2 Climatology

The annual standardized anomalies are calculated by monthly values subtract the given annual mean then divided by the given annual standardized deviation; Climatological annual standardized anomalies are defined as the monthly average of the annual standardized anomalies. The spatial distribution of TWS and TWSC climatological annual standardized anomalies derived from ERA-Interim and GLDAS-Noah are shown in Figs. 4 and 5, respectively. The performance of ERA-Interim and GLDAS-Noah might vary greatly due to insufficient physical interpretation of land-surface processes (Niu and Yang, 2006; Zeng et al., 2008). However, the spatial patterns reveal strong consistencies.

After suffering consistent drought in the winter (December–February), the southeast corner of the Yangtze basin starts to get wet during March–May, due mainly to the South China rainfall belt extension and the mean precipitation increase in the lower basin (Ding and Chan, 2005; Qian et al., 2002). High positive TWS standardized anomalies emerge in most of the Yangtze basin during June–October (Fig. 4), and large increase in July compared to June (Fig. 5), which corresponds to the intensive precipitation observed along the whole Yangtze River from mid-June to mid-July (Ding,





HESSD
9, 11487–11520, 2012

1992), which is also called the Meiyu in China. It is noted that negative TWS standardized anomalies still exist in the center part (around 107° E) from ERA-Interim which is different from the negative GLDAS-Noah value in the upper area. According to the climatological rainfall differences between June and May and between July and June (Qian et al., 2002, Fig. 4), the increased rainfall in June compared to that in May appears in the Plateau and Southwest China with the center in the upper Yangtze reach.

Another area of increased rainfall is along the eastern coastland with the center in the lower Yangtze reach, and there is no obvious increase of rainfall in the central part of China. In July compared to June, the increased rainfall has migrated to the north of the lower Yangtze River basin while the rainfall is steadily increasing at the upper parts. This precipitation change pattern during May–July resembles remarkably with the TWS pattern derived from ERA-Interim (Fig. 4). After July, the TWS anomalies in the middle and lower Yangtze reach is decreasing sharply, while keep quite high positive till October in the upper Yangtze reach, mainly due to the rainy season from mid-June to mid-September without intermission.

This striking consistency between TWS and rainfall pattern is not unexpected. Higher precipitation leading to higher soil moisture can generally be considered trivial, though there are a few exceptions. For instance in the cases of intense precipitation with rates beyond the infiltration rate or precipitation over very wet or saturated areas, the rainfall anomalies will result in runoff anomalies rather than soil moisture (Dunne, 1978; Horton, 1933). Nevertheless, except for few extreme cases, there is an obvious and direct response of soil moisture to precipitation. On the other hand, the feedback via the return path from soil moisture through evapotranspiration to precipitation would also play an important role in the TWS variability, even though is weaker and subtler (Seneviratne et al., 2010). Numerous previous researches (Dirmeyer, 2011; Jung et al., 2010; Wei et al., 2012) show that the Yangtze River basin is dominated by wet soil moisture regimes, where soil moisture does not mainly control the evapotranspiration variability and have a weak impact on the change of rainfall. Dirmeyer (2011) also confirm that the soil moisture does not typically exert a feedback on the atmosphere or have a damping effect on climate variability. Thus, it is reasonable to speculate that the TWS variability in the Yangtze River basin is mainly controlled by the large-scale atmosphere circulations, which is also proved by Wei et al. (2012). Moreover, as displayed in Fig. 4, the Yangtze River basin suffered highest TWS anomalies during June–July, which also implies high flood risks during these this period, since runoff is sensitive to soil moisture content under wet soil regimes, as soil moisture is very wet and reach its saturation, high precipitation variability may lead to high runoff variability that cannot be damped by soil moisture storage (Seneviratne et al., 2010).

It should be recognized that the TWS pattern in the upper reach is completely different from that in middle and lower Yangtze reaches, which may be explained by the various large-scale circulations and heterogeneous land-surface conditions. The upper Yangtze reach is mainly influenced by the South Asian (or Indian) summer monsoon, and the middle and lower Yangtze reach is controlled by East Asian summer monsoon (Ding and Chan, 2005). The seasonal march of the Asian summer monsoon plays a crucial role in heat and moisture transport and hydrological cycle, and related rainfall systems performs differently in the upper reaches than the middle and lower reaches (Qian et al., 2002). As the topography in the upper Yangtze reach is totally different than that in the middle and lower reach (Fig. 1), the land-surface heterogeneities in temperature is expected (Giorgi et al., 1997; Salama et al., 2012), and also, the land covers and hydrological conditions are different in these two reaches (Piao et al., 2010). The inhomogeneous land-surface results in the heterogeneity of the surface energy partitioning which impacts the land-surface interactions (Brunsell et al., 2011; Ma et al., 2008). Therefore, the different responses of land-surface systems are expected in the upper Yangtze reach and middle-lower reach, respectively. For example, soil moisture exerts a significant positive control on the maximum temperature and mean temperature in the middle-lower reach during summer, while no significant control on the upper reach. Furthermore, while the positive sign dominates the soil moisture-precipitation coupling in the upper Yangtze reach, the negative sign exists in the middle and lower Yangtze reach (Zhang et al., 2011).





HESSD
9, 11487–11520, 2012

## 5.3 TWS trends analysis

Jung et al. (2010) pointed out that the major El Niño event in 1998 was followed by changes in the behavior of some land water cycle components, such as SM. Additionally, GLDAS-Noah outputs show obvious errors in 1996 and 1997. Therefore, we separate the whole period to two parts, from January 1979 to December 1995 and from January 1998 to December 2010. Both ERA-Interim and GLDAS-Noah datasets shows decreasing TWS trends over large parts of the Yangtze River basin between 1998 and 2010 which match the descending trend of soil moisture from the microwave satellite observations between 1998 to 2008 (Jung et al., 2010). In Fig. 6, ERA-Interim datasets shows significant decreasing trends (most of which pass the 95 % and some pass the 99 % confidence level) in the middle and lower reaches which reaches a maximum of $-3.93\,\mathrm{mm\,yr^{-1}}$, while the upper reach suffers milder decreases and also insignificant trends in some parts during the period between 1998–2010. However, GLDAS-Noah datasets have a faster decrease (most pass the 99 % confidence level) in upper reaches than the middle and lower reaches of the basin, which reaches a maximum of $-12.6\,\mathrm{mm\,yr^{-1}}$, but insignificant trends exist both in the upper reach and the middle and lower reaches. Between 1979 and 1995, there are decreasing trends in the head of the basin from both ERA-Interim and GLDAS-Noah datasets. Most regions of the basin shows insignificant trend in ERA-Interim, while there are upward trends in some of the upper Yangtze and downward trends in some part of middle and lower Yangtze. It is noted that most grid points, especially in the middle and lower basin, show significant negative trends in both datasets, even though their rates are disparate. This result indicates that the Yangtze River basin is drying up, which have been also announced by a new WWF study (http://www.asianscientist.com/topnews/yangtze-river-basin-is-drying-up-wwf-china-2012/).

Monthly climatology standardized anomalies of TWS are calculated by monthly TWS minus the corresponding monthly value of annual cycle and then dividing by the standard deviation of the values of the same months within the period 1979–2010, in order





HESSD
9, 11487–11520, 2012

to eliminate the influence of inter annual variability for intra annual analysis. As discussed before, ERA-Interim dataset has better accuracy, at least, in the upper reach of the Yangtze River and GLDAS-Noah outputs have notable error in 1996 and 1998. Therefore, only ERA-Interim dataset is used in this section.

MKS test is employed to detect the transition points in the temporal behavior of TWS standardized anomalies. From Fig. 7, generally speaking, spatial averaged TWS standardized anomaly trends are not significant (< 95 % confidence level) and not monotonic (i.e. with a transition point) during the period of 1979–2010. From the whole basin and the annual perspective, 2006 is detected as the only transition point during the 32-yr period of 1979–2010 at which the TWS standardized anomalies began to decrease sharply and this trend reaches the 95 % confidence level in 2010. The transition point occurs one year earlier in the flood season, whereas two years later in the dry season. In the middle and lower Yangtze reaches, transition points occur around 2005 both in flood season and dry season. It is noted that there is a significant downward trend in 2009 and 2010 after 4 yr insignificant decrease which was the first time to happen from 1979 onwards. In the upper Yangtze reach, TWS standardized anomalies experience mainly downward trends in the wet season of last 3 decades, whereas increasing trends in the dry season. In addition, transition points occur several times (1982, 1989, 1995, 2001, 2005) and in the period of 1986–1988, the decrease is significant in the flood season in the upper Yangtze reach. We also examine the transition points through MKS of the TWS standardized anomalies in the middle and lower Yangtze reaches during June–July, and the result is exactly the same as that in the flood season, though the TWS standardized anomalies show difference from each other.

From Figs. 7 and 8, it can be seen clearly that the last 6-yr period (2005–2010) was the driest period of the Yangtze River basin (especially in the middle and lower reaches) since 1979. This result is quite consistent with the severe drought events of the basin documented by other researches, as Wei et al. (2012) documented that the Yangtze River basin suffered one of the driest rain seasons during the 32-yr period of 1979–2010 in 2005, and Yan et al. (2007) addressed a widespread drought





HESSD
9, 11487–11520, 2012

occurred over the southwestern part of the basin in the spring which was the most serious one since 1979 in the same year. Then the worst drought in more than century struck Southwest China and Sichuan in the summer of 2006, and Dai et al. (2008) showed that the middle and lower of Yangtze River reached its lowest in the last 50 yr in the flood season. In 2007, the area around the Yangtze River suffered a severe drought again. In some places water levels of the river dropped to their lowest levels since records began 142 yr ago. The drought was also severe in large areas of the normally wet south. Reservoirs and rivers shrunk and supplies of drinking water fell to alarmingly low levels. The extreme drought of 2009/2010 over Southwestern Yangtze (including Yunnan, Sichuan and Guizhou) is the driest meteorological event with the lowest percentage rainfall anomaly and the longest rain-free period during winter season (October–February) in the past 50 yr, and also the severest one with the lowest percentage rainfall anomaly at the same period since 1880 which had been documented by Yang et al. (2012). In 2011, some part of Yangtze Delta where is usually considered as one of the lushest in China experienced the worst drought for more than 100 yr (http://factsanddetails.com/china.php?itemid=1879&catid=10&subcatid=64).

Monthly climatology standardized anomalies of precipitation from ERA-Interim, GPCC and PREC/L has been computed and compared to monthly climatology standardized anomalies of TWS (not shown here), to examine the correlation between them. The correlations between TWS climatology anomalies from ERA-Interim and precipitation climatology anomalies from ERA-Interim, GPCC and PREC/L of the Yangtze basin in the wet season are all pretty high (0.69, 0.53 and 0.49, respectively), while much lower, especially for GPCC and PREC/L, in the dry season (0.48, 0.21 and 0.25, respectively). From regional perspective, the middle and lower Yangtze reaches has been examined having larger agreement between TWS from ERA-Interim and precipitation from these three datasets than that of upper Yangtze reach. The notable negative TWS anomalies in the middle and lower Yangtze reaches are in good agreement with the significant decrease of precipitation from ERA-Interim in the last 6 yr; GPCC and PREC/L have more gentle precipitation negative anomalies in this period and not





HESSD
9, 11487–11520, 2012

shown any special comparing to the period earlier(not shown here). These differences can also been seen clearly from Fig. 3, where there is a clear downward shift for ERA-Interim relative to both GPCC and PREC/L in last 6 yr. This shift is in good agreement in the general decline in values relative to GPCC for the latest decade, which may be caused by too low Sea Surface Temperature (SST) of ERA-Interim, or fewer stations in the GPCC archive for recent years (Simmons et al., 2010). PREC/L use fewer gauging stations data since 1990s as well, thus it is difficult to assess the recent huge and sudden drop in ERA-Interim only comparing to GPCC and PREC/L. However, the dramatic precipitation decrease in the middle and lower Yangtze reaches had been examined by Zhu et al. (2011, Fig. 2) over the last decade (2000–2008), and the rainfall anomalies based on 160-station precipitation dataset of the last 58 yr (1951–2008) dropped shapely from positive to negative values around 2004. This pattern of the precipitation is consistent with the dramatic decrease of precipitation from ERA-Interim from positive to negative values from 2004 in the middle and lower Yangtze reaches (Fig. 3), suggesting that the recent drop of precipitation is most likely the biggest contributor of the massive decline of TWS in the middle and lower Yangtze reaches. Ding et al. (2008) pointed out that the recent change in the summer rainfall pattern in the Yangtze River is highly related to the variability of the East Asian Summer Monsoon (EASM) through the moisture transport and supply. Zhu et al. (2011) addressed that the eastward recession of the Western Pacific Subtropical High and the significant changes of the global SST are mainly responsible for the rainfall deficit of the Yangtze River basin after 2000. Yan et al. (2007) and Liu et al. (2007) documented that the intensification and westward shift of the WPSH and the easterly anomaly over Northern Indian Ocean are two key causes of 2005-spring drought over the Southwestern China. The northward shift of WPSH and the negative snow cover anomaly over Tibet Plateau are important contributors for the 2006-summer drought (Zou and Gao, 2007; Li et al., 2009). The extreme drought event of 2009/2010 over Southwestern China is associated with the westward extension of WPSH due to the Arabian Sea cyclonic anomaly and the El Niño Modoki event during 2009/2010. As we mentioned in Sect. 5.2, the soil moisture in the Yangtze





HESSD
9, 11487–11520, 2012
Analysis of long-term terrestrial water storage variations
Y. Huang et al.

River has weak impact on the atmosphere, so it is reasonable to speculate that the temporal behaviors of the TWS in the Yangtze River basin are mainly due to the variations of large-scale circulations.

Since ERA-Interim TWS products do not include the impacts of the human activities such as the TGD and land cover change in the model structure but rather in the assimilated observations, the effects on the regional climate in the Yangtze River basin is not that obvious. However, some studies have demonstrated the human impacts on the Yangtze River basin. For examples, Dai et al. (2008); Yang et al. (2010) show that TGD reservoirs could have a direct impact on the intra-annual changes of the downstream Yangtze discharges, leading to dumping the seasonal variations of Yangtze River discharge in the middle and lower reaches. Miller et al. (2005); Wu et al. (2006) also documented that the land use change associated with the TGD would alter regional pattern of precipitation, wind and temperature. It could impact the hydrological cycle of the river basin, may also lead to the changes of the soil-climate interaction strength which probably alter the current dumping effect of soil wetness on the climate variability. There has been no irrefutable evidence to prove that TGR is highly related to the driest period occurred in last several years due to the short period of TGD operation. However, as showed in Figs. 7 and 8, the consistent droughts in the recent years and the operation of TGR occurred simultaneously. In 2003, the water level of TGR reached 135 m, coincidently in 2004, the middle and lower Yangtze started its driest period in the last 32 yr. Also, the whole basin suffered an abrupt change in 2006, when TGD was impounded from 135 m to 156 m. This coincidence is very striking and may imply the possible connection between TGD and the consistent drought in recent years. Except TGR, numerous reservoirs within the Yangtze catchment has reached 200 $km^3$ (Yang et al., 2005), more than five times the storage capacity of TGR, the impacts of these reservoirs on TWS cannot be neglected. The Yangtze basin has witnessed remarkable changes in land use and cover induced by high population density and rapid but uneven economic growth (Long et al., 2007; Yin et al., 2010). These changes might alter the soil properties and soil-climate interactions which probably have great influence on the





HESSD
9, 11487–11520, 2012

TWS and runoff distribution. It should be pointed out that the ERA-Interim TWS might contain significant uncertainties because it relies heavily on satellites observations and modeling. Further investigations and analyses are needed to assess the significant impacts of these human activities on the TWS of the Yangtze River basin.

## 6 Conclusions

This study analyzes the spatial and temporal variations of the TWS in the Yangtze River basin during the period of 1979–2010 based on ERA-Interim and GLDAS-Noah. After comparing to the field measurements data, ERA-Interim is found to perform better in the Yangtze River basin than GLDAS-Noah. Linear regression and MK test have been used to detect trends and the significance of trends in the TWS at each pixel of the whole basin. In addition, the MKS test has been used to detect transition points in the temporal series of the spatially averaged TWS annual standardized anomalies in the upper, middle-lower and whole basin, respectively. We conclude that the TWS variations over the Yangtze River basin during the period of 1979–2010 have the following characteristics:

1. Most of the Yangtze basin exhibits the highest positive TWS anomalies during June–July, mainly due to the Meiyu rain event. This intensified rainfall not only results in the very high positive TWS anomalies, but probably also lead to high runoff anomalies which cause the floods over the basin.

2. The Yangtze River basin is drying up, especially after the year 1998. The TWS variation is good correlated with the precipitation variation from ERA-Interim, GPCC and PREC/L, especially in the wet season and the middle and lower reaches, suggesting the TWS variation is mainly controlled by the precipitation.

3. In the middle and lower Yangtze reaches, TWS behavior changed abruptly and started to decrease in 2004. Coincidently, the TGR started impoundment in 2003.





HESSD
9, 11487–11520, 2012

From a basin and annual perspective, 2006 is detected as the only transition point initiating TWS to suffer high negative anomalies, while the TGR raised its water level from 135 m to 156 m in the same year. Due to the short period of the TGD impoundment, it is really hard to prove a link of TGR with the consistent drought in recent years, but the coincidence suggests a possible connection.

4. The last 6-yr period (2005–2010) was the driest period in terms of TWS of the Yangtze River basin (especially in the middle and lower Yangtze reaches) since 1979, which is mainly a result of the dramatic decrease of the precipitation, might also impacted by human activities.

*Acknowledgements.* Ying Huang acknowledges support from Chinese Scholarship Council (CSC). We are grateful for the advices and suggestions of Xuebin Zhang and Kun Yang.

## References

Berrisford, P., Dee, D., Poli, P., Brugge, R., Fielding, K., Fuentes, M., Kållberg, P., Kobayashi, S., Uppala, S., and Simmons, A.: The ERA-Interim archive, version 2.0, ERA report series 1, ECWMF, UK, 2011. 11491

Brunsell, N. A., Mechem, D. B., and Anderson, M. C.: Surface heterogeneity impacts on boundary layer dynamics via energy balance partitioning, Atmos. Chem. Phys., 11, 3403–3416, doi:10.5194/acp-11-3403-2011, 2011. 11499

Chen, J. L., Rodell, M., Wilson, C. R., and Famiglietti, J. S.: Low degree spherical harmonic influences on Gravity Recovery and Climate Experiment (GRACE) water storage estimates, Geophys. Res. Lett., 32, L14405, doi:10.1029/2005gl022964, 2005. 11490

Chen, J. L., Wilson, C. R., Tapley, B. D., Yang, Z. L., and Niu, G. Y.: 2005 drought event in the Amazon River basin as measured by GRACE and estimated by climate models, J. Geophys. Res., 114, B05404, doi:10.1029/2008jb006056, 2009. 11494

Chen, M., Xie, P., Janowiak, J. E., and Arkin, P. A.: Global land precipitation: a 50-yr monthly analysis based on gauge observations, J. Hydrometeorol., 3, 249–266, doi:10.1175/1525-7541(2002)003<0249:glpaym>2.0.co;2, 2002. 11493

Dai, Z., Du, J., Li, J., Li, W., and Chen, J.: Runoff characteristics of the Changjiang River during 2006: Effect of extreme drought and the impounding of the Three Gorges Dam, Geophys. Res. Lett., 35, L07406, doi:10.1029/2008gl033456, 2008. 11490, 11502, 11504
Dee, D. P., Uppala, S. M., Simmons, A. J., Berrisford, P., Poli, P., Kobayashi, S., Andrae, U., Balmaseda, M. A., Balsamo, G., Bauer, P., Bechtold, P., Beljaars, A. C. M., van de Berg, L., Bidlot, J., Bormann, N., Delsol, C., Dragani, R., Fuentes, M., Geer, A. J., Haimberger, L., Healy, S. B., Hersbach, H., Hólm, E. V., Isaksen, L., Kållberg, P., Köhler, M., Matricardi, M., McNally, A. P., Monge-Sanz, B. M., Morcrette, J. J., Park, B. K., Peubey, C., de Rosnay, P., Tavolato, C., Thépaut, J. N., and Vitart, F.: The ERA-Interim reanalysis: configuration and performance of the data assimilation system, Q. J. Roy. Meteor. Soc., 137, 553–597, doi:10.1002/qj.828, 2011. 11492
Ding, Y. H.: Summer monsoon rainfalls in China, J. Meteorol. Soc. Jpn., 70, 373–396, 1992. 11497
Ding, Y. H. and Chan, J. C. L.: The East Asian summer monsoon: an overview, Meteorol. Atmos. Phys., 89, 117–142, doi:10.1007/s00703-005-0125-z, 2005. 11497, 11499
Ding, Y. H., Wang, Z., and Sun, Y.: Inter-decadal variation of the summer precipitation in East China and its association with decreasing Asian summer monsoon. Part I: Observed evidences, Int. J. Climatol., 28, 1139–1161, doi:10.1002/joc.1615, 2008. 11503
Ding, Y. H., Sun, Y., Wang, Z., Zhu, Y., and Song, Y.: Inter-decadal variation of the summer precipitation in China and its association with decreasing Asian summer monsoon Part II: Possible causes, Int. J. Climatol., 29, 1926–1944, doi:10.1002/joc.1759, 2009. 11489
Dirmeyer, P. A.: The terrestrial segment of soil moisture-climate coupling, Geophys. Res. Lett., 38, L16702, doi:10.1029/2011gl048268, 2011. 11498
Dorigo, W. A., Scipal, K., Parinussa, R. M., Liu, Y. Y., Wagner, W., de Jeu, R. A. M., and Naeimi, V.: Error characterisation of global active and passive microwave soil moisture datasets, Hydrol. Earth Syst. Sci., 14, 2605–2616, doi:10.5194/hess-14-2605-2010, 2010. 11496, 11497
Dorigo, W. A., Wagner, W., Hohensinn, R., Hahn, S., Paulik, C., Xaver, A., Gruber, A., Drusch, M., Mecklenburg, S., van Oevelen, P., Robock, A., and Jackson, T.: The International Soil Moisture Network: a data hosting facility for global in situ soil moisture measurements, Hydrol. Earth Syst. Sci., 15, 1675–1698, doi:10.5194/hess-15-1675-2011, 2011. 11496
Dunne, T.: Field studies of hillslope flow processes, in: Hillslope Hydrology, edited by: Kirkby, M. J., Wiley-Interscience, New York, 227–293, 1978. 11498





HESSD
9, 11487–11520, 2012

Entekhabi, D., Njoku, E. G., O'Neill, P. E., Kellogg, K. H., Crow, W. T., Edelstein, W. N., Entin, J. K., Goodman, S. D., Jackson, T. J., Johnson, J., Kimball, J., Piepmeier, J. R., Koster, R. D., Martin, N., McDonald, K. C., Moghaddam, M., Moran, S., Reichle, R., Shi, J. C., Spencer, M. W., Thurman, S. W., Leung, T., and Van Zyl, J.: The Soil Moisture Active Passive (SMAP) mission, Proc. IEEE, 98, 704–716, doi:10.1109/jproc.2010.2043918, 2010. 11489

Famiglietti, J. S.: Remote sensing of terrestrial water storage, soil moisture and surface waters, in: The State of the Planet: Frontiers and Challenges in Geophysics, Geophysical Monograph Series, 150, edited by: Sparks, R. S. J. and Hawkesworth, C. J., AGU, Washington, DC, USA, 197–207, 2004. 11488

Famiglietti, J. S., Ryu, D., Berg, A. A., Rodell, M., and Jackson, T. J.: Field observations of soil moisture variability across scales, Water Resour. Res., 44, W01423, doi:10.1029/2006wr005804, 2008. 11489

Giorgi, F., Hurrell, J. W., Marinucci, M. R., and Beniston, M.: Elevation dependency of the surface climate change signal: a model study, J. Climate, 10, 288–296, doi:10.1175/1520-0442(1997)010<0288:edotsc>2.0.co;2, 1997. 11499

Horton, R. E.: The role of infiltration in the hydrologic cycle, EOS T. Am. Geophys. Un., 14,446–460,1933. 11498

IPCC: Climate Change 2001: The Scientific Basis. Contribution of Working Group I to the Third Assessment Report of the Intergovernmental Panel on Climate Change, edited by: Houghton, J. T., Ding, Y., Griggs, D. J., Noguer, M., van der Linden, P. J., Dai, X., Maskell, K., and Johnson, C. A., Cambridge University Press, Cambridge, United Kingdom and New York, NY, USA, 881 pp., 2001. 11490

Jung, M., Reichstein, M., Ciais, P., Seneviratne, S. I., Sheffield, J., Goulden, M. L., Bonan, G., Cescatti, A., Chen, J., de Jeu, R., Dolman, A. J., Eugster, W., Gerten, D., Gianelle, D., Gobron, N., Heinke, J., Kimball, J., Law, B. E., Montagnani, L., Mu, Q., Mueller, B., Oleson, K., Papale, D., Richardson, A. D., Roupsard, O., Running, S., Tomelleri, E., Viovy, N., Weber, U., Williams, C., Wood, E., Zaehle, S., and Zhang, K.: Recent decline in the global land evapotranspiration trend due to limited moisture supply, Nature, 467, 951–954, 2010. 11498, 11500

Kendall, M. G.: Rank Correlation Measures, Charles Griffin, London, 1975. 11495

Li, C., Yang, Z., and Wang, X.: Trends of annual natural runoff in the Yellow River basin, Water Int., 29, 447–454, doi:10.1080/02508060408691807, 2004. 11495





HESSD

9, 11487–11520, 2012

Analysis of long-term terrestrial water storage variations

Y. Huang et al.

Title Page
Abstract | Introduction
Conclusions | References
Tables | Figures
Back | Close
Full Screen / Esc
Printer-friendly Version
Interactive Discussion

Li, L.-J., Zhang, L., Wang, H., Wang, J., Yang, J.-W., Jiang, D.-J., Li, J.-Y., and Qin, D.-Y.: Assessing the impact of climate variability and human activities on streamflow from the Wuding River basin in China, Hydrol. Process., 21, 3485–3491, doi:10.1002/hyp.6485, 2007. 11495

Li, Y. H., Xu, H. M., and Liu, D.: Features of the extremely severe drought in the east of Southwest China and anomalies of atmospheric circulation in summer 2006, Acta Meterol. Sin., 67, 122–132, 2009 (in Chinese). 11503

Liu, Y., Zhao, E. X., Peng, G. F., and Yang, S. Q.: Severe drought in the early summer of 2005 in Yunnan and middle-high latitudes circulation, Arid. Meteor., 25, 32–37, 2007 (in Chinese). 11503

Liu, Y. Y., Parinussa, R. M., Dorigo, W. A., De Jeu, R. A. M., Wagner, W., van Dijk, A. I. J. M., McCabe, M. F., and Evans, J. P.: Developing an improved soil moisture dataset by blending passive and active microwave satellite-based retrievals, Hydrol. Earth Syst. Sci., 15, 425–436, doi:10.5194/hess-15-425-2011, 2011. 11497

Long, H., Heilig, G. K., Li, X., and Zhang, M.: Socio-economic development and land-use change: analysis of rural housing land transition in the transect of the Yangtse River, China, Land Use Policy, 24, 141–153, doi:10.1016/j.landusepol.2005.11.003, 2007. 11504

Ma, Y., Menenti, M., Feddes, R., and Wang, J.: Analysis of the land surface heterogeneity and its impact on atmospheric variables and the aerodynamic and thermodynamic roughness lengths, J. Geophys. Res., 113, D08113, doi:10.1029/2007jd009124, 2008. 11499

Mann, H. B.: Nonparametric tests against trend, Econometrica, 13, 245–259, 1945. 11495

Miller, N. L., Jin, J., and Tsang, C.-F.: Local climate sensitivity of the Three Gorges Dam, Geophys. Res. Lett., 32, L16704, doi:10.1029/2005gl022821, 2005. 11504

Moraes, J. M., Pellegrino, G. Q., Ballester, M. V., Martinelli, L. A., Victoria, R. L., and Krusche, A. V.: Trends in hydrological parameters of a Southern Brazilian watershed and its relation to human induced changes, Water Resour. Manag., 12, 295–311, doi:10.1023/a:1008048212420, 1998. 11495

Niu, G.-Y. and Yang, Z.-L.: Assessing a land surface model's improvements with GRACE estimates, Geophys. Res. Lett., 33, L07401, doi:10.1029/2005gl025555, 2006. 11488, 11497

Piao, S., Ciais, P., Huang, Y., Shen, Z., Peng, S., Li, J., Zhou, L., Liu, H., Ma, Y., Ding, Y., Friedlingstein, P., Liu, C., Tan, K., Yu, Y., Zhang, T., and Fang, J.: The impacts of climate change on water resources and agriculture in China, Nature, 467, 43–51, 2010. 11499





HESSD
9, 11487–11520, 2012

Analysis of long-term terrestrial water storage variations

Y. Huang et al.

Qian, W., Kang, H. S., and Lee, D. K.: Distribution of seasonal rainfall in the East Asian monsoon region, Theor. Appl. Climatol., 73, 151–168, doi:10.1007/s00704-002-0679-3, 2002. 11497, 11498, 11499

Rodell, M., Famiglietti, J. S., Chen, J., Seneviratne, S. I., Viterbo, P., Holl, S., and Wilson, C. R.: basin scale estimates of evapotranspiration using GRACE and other observations, Geophys. Res. Lett., 31, L20504, doi:10.1029/2004gl020873, 2004. 11494

Rui, H.: README Document for Global Land Data Assimilation System Version 1 (GLDAS-1) Products, Goddard Earth Sciences Data and Information Services Center, NASA, USA, 2011. 11492

Salama, M., Van der Velde, R., Zhong, L., Ma, Y., Ofwono, M., and Su, Z.: Decadal variations of land surface temperature anomalies observed over the Tibetan Plateau by the Special Sensor Microwave Imager (SSM/I) from 1987 to 2008, Climatic Change, 114, 769–781, doi:10.1007/s10584-012-0427-3, 2012. 11499

Schneider, U., Becker, A., Meyer-Christoffer, A., Ziese, M., and Rudolf, B.: Global Precipitation Analysis Products of the GPCC, Global Precipitation Climatology Centre (GPCC), Deutscher Wetterdienst, Offenbach a.M., Germany, 2011. 11493

Scipal, K., Holmes, T., de Jeu, R., Naeimi, V., and Wagner, W.: A possible solution for the problem of estimating the error structure of global soil moisture data sets, Geophys. Res. Lett., 35, L24403, doi:10.1029/2008gl035599, 2008. 11496, 11497

Seneviratne, S. I., Viterbo, P., Lüthi, D., and Schär, C.: Inferring Changes in Terrestrial Water Storage Using ERA-40 Reanalysis Data: The Mississippi River basin, J. Climate, 17, 2039–2057, doi:10.1175/1520-0442(2004)017<2039:icitws>2.0.co;2, 2004. 11490

Seneviratne, S. I., Corti, T., Davin, E. L., Hirschi, M., Jaeger, E. B., Lehner, I., Orlowsky, B., and Teuling, A. J.: Investigating soil moisture–climate interactions in a changing climate: a review, Earth-Sci. Rev., 99, 125–161, doi:10.1016/j.earscirev.2010.02.004, 2010. 11489, 11498, 11499

Simmons, A., Uppala, S., Dee, D., and Kobayashi, S.: ERA-Interim: new ECMWF reanalysis products from 1989 onwards, ECMWF Newsletter, 110, 26–35, 2006. 11491

Simmons, A. J., Willett, K. M., Jones, P. D., Thorne, P. W., and Dee, D. P.: Low-frequency variations in surface atmospheric humidity, temperature, and precipitation: Inferences from reanalyses and monthly gridded observational data sets, J. Geophys. Res., 115, D01110, doi:10.1029/2009jd012442, 2010. 11503

Sneyers, R.: Sur l'analyse statistique des séries d'observations, Secrétariat de l'Organisation Météorologique Mondiale, Genève, 1975. 11495

Syed, T. H., Famiglietti, J. S., Rodell, M., Chen, J., and Wilson, C. R.: Analysis of terrestrial water storage changes from GRACE and GLDAS, Water Resour. Res., 44, W02433, doi:10.1029/2006wr005779, 2008. 11490, 11494

Tapley, B. D., Bettadpur, S., Watkins, M., and Reigber, C.: The gravity recovery and climate experiment: mission overview and early results, Geophys. Res. Lett., 31, L09607, doi:10.1029/2004gl019920, 2004a. 11489

Tapley, B. D., Bettadpur, S., Ries, J. C., Thompson, P. F., and Watkins, M. M.: GRACE measurements of mass variability in the Earth system, Science, 305, 503–505, doi:10.1126/science.1099192, 2004b. 11489

van der Velde, R., Su, Z., and Ma, Y.: Impact of soil moisture dynamics on ASAR $\sigma^o$ signatures and its spatial variability observed over the Tibetan Plateau, Sensors, 8, 5479–5491, 2008. 11489

Viterbo, P. and Beljaars, A. C. M.: An improved land surface parameterization scheme in the ECMWF model and its validation, J. Climate, 8, 2716–2748, 1995. 11491

Wang, H.-L., Liu, J., and Kuang, X.-Y.: Comparison of four reanalysis precipitation datasets and observation over the middle lower reaches of the Yangtze River, Resour. Environ. Yangtze basin, 17, 5, 703–711, 2008, (in Chinese). 11493

Wei, J., Dirmeyer, P. A., Bosilovich, M. G., and Wu, R.: Water vapor sources for Yangtze River Valley rainfall: Climatology, variability, and implications for rainfall forecasting, J. Geophys. Res., 117, D05126, doi:10.1029/2011jd016902, 2012. 11498, 11499, 11501

Wong, C. M., Williams, C. E., Pittock, J., Collier, U., and Schelle, P.: World's top 10 rivers at risk, WWF International, Gland, Switzerland, 2007. 11490

Wu, L., Zhang, Q., and Jiang, Z.: Three Gorges Dam affects regional precipitation, Geophys. Res. Lett., 33, L13806, doi:10.1029/2006gl026780, 2006. 11504

Yan, H.-M., Duan, X., and Cheng, J.-G.: Study on a severe drought event over Yunnan in spring 2005, J. Trop. Meteorol., 23, 300–306, 2007 (in Chinese). 11501, 11503

Yang, J., Gong, D., Wang, W., Hu, M., and Mao, R.: Extreme drought event of 2009/2010 over Southwestern China, Meteorol. Atmos. Phys., 115, 173–184, doi:10.1007/s00703-011-0172-6, 2012. 11502





HESSD

9, 11487–11520, 2012

Analysis of long-term terrestrial water storage variations

Y. Huang et al.

Title Page
Abstract | Introduction
Conclusions | References
Tables | Figures
◀| |▶
◀ ▶
Back | Close
Full Screen / Esc
Printer-friendly Version
Interactive Discussion

Yang, S. L., Zhang, J., Zhu, J., Smith, J. P., Dai, S. B., Gao, A., and Li, P.: Impact of dams on Yangtze River sediment supply to the sea and delta intertidal wetland response, J. Geophys. Res., 110, F03006, doi:10.1029/2004jf000271, 2005. 11504

Yang, S. L., Liu, Z., Dai, S. B., Gao, Z. X., Zhang, J., Wang, H. J., Luo, X. X., Wu, C. S., and Zhang, Z.: Temporal variations in water resources in the Yangtze River (Changjiang) over the Industrial Period based on reconstruction of missing monthly discharges, Water Resour. Res., 46, W10516, doi:10.1029/2009wr008589, 2010. 11504

Yin, R., Xiang, Q., Xu, J., and Deng, X.: Modeling the Driving Forces of the Land Use and Land Cover Changes Along the Upper Yangtze River of China, Environ. Manage., 45, 454–465, doi:10.1007/s00267-009-9377-6, 2010. 11504

Zaitchik, B. F., Rodell, M., and Olivera, F.: Evaluation of the Global Land Data Assimilation System using global river discharge data and a source-to-sink routing scheme, Water Resour. Res., 46, W06507, doi:10.1029/2009wr007811, 2010. 11496

Zeng, N., Yoon, J.-H., Mariotti, A., and Swenson, S.: Variability of basin-scale terrestrial water storage from a per water budget method: the amazon and the Mississippi, J. Climate, 21, 248–265, doi:10.1175/2007jcli1639.1, 2008. 11497

Zhang, J., Wu, L., and Dong, W.: land-atmosphere coupling and summer climate variability over East Asia, J. Geophys. Res., 116, D05117, doi:10.1029/2010jd014714, 2011. 11499

Zhong, L., Ma, Y., Salama, M., and Su, Z.: Assessment of vegetation dynamics and their response to variations in precipitation and temperature in the Tibetan Plateau, Climatic Change, 103, 519–535, doi:10.1007/s10584-009-9787-8, 2010. 11494

Zhu, Y., Wang, H., Zhou, W., and Ma, J.: Recent changes in the summer precipitation pattern in East China and the background circulation, Clim. Dynam., 36, 1463–1473, doi:10.1007/s00382-010-0852-9, 2011. 11503

Zou, X. K. and Gao, H.: Analysis of severe drought and heat wave over the Sichuan Basin in the summer of 2006, Adv. Clim. Chang. Res., 3, 149–153, 2007 (in Chinese). 11503

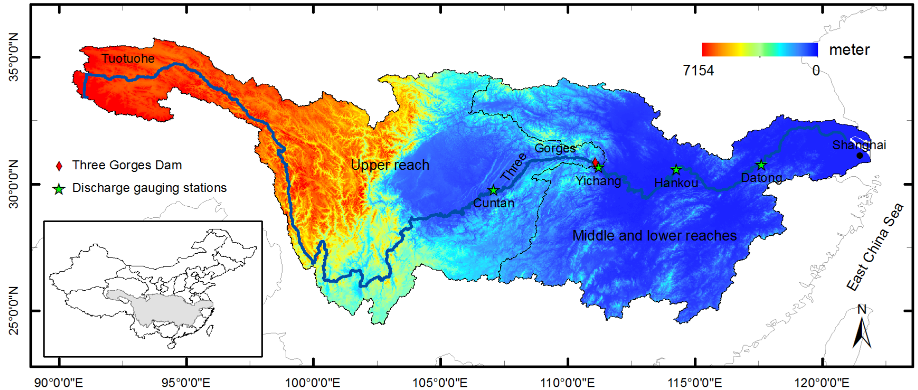


**Fig. 1.** Elevation map of the study area, the Yangtze River basin. The green stars are the locations of the main gauging stations. The position of the TGD is shown as the red diamond.

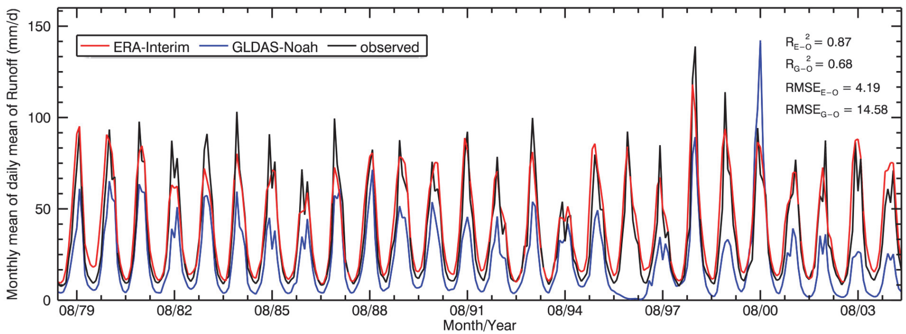


**Fig. 2.** Spatial averaged time series of ERA-Interim estimated (red curve), GLDAS-Noah estimated (blue curve) and observed (black curve) runoff of upper Yangtze reach between January 1979 and December 2004.





HESSD
9, 11487–11520, 2012

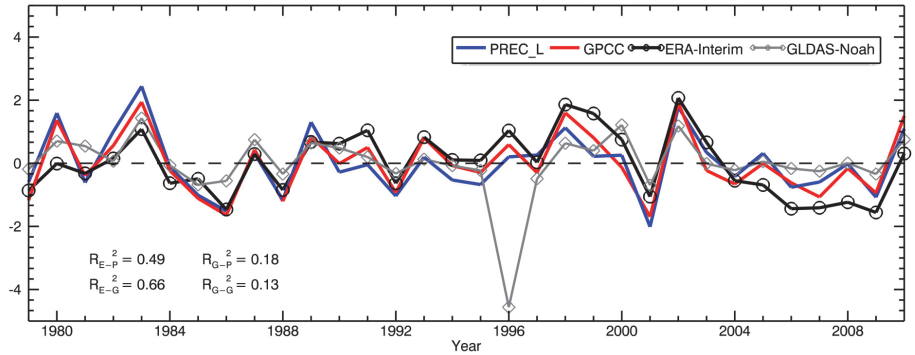


**Fig. 3.** Spatial averaged time series of standardized anomalies of annual precipitation in the middle and lower Yangtze reaches based on PREC/L (blue curve), GPCC (red curve), ERA-Interim (black circle curve) and GLDAS-Noah (gray diamond curve) from 1979 to 2010.





HESSD
9, 11487–11520, 2012

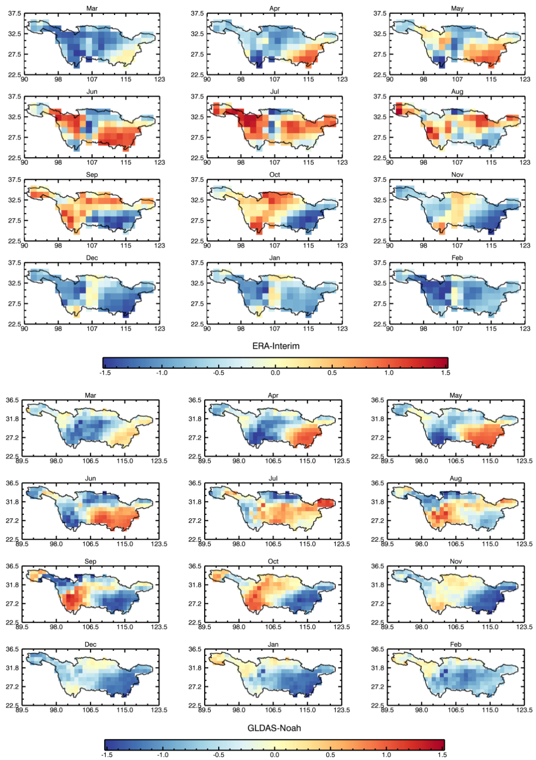


**Fig. 4.** Spatial patterns of monthly averaged TWS annual standardized anomalies from ERA-Interim computed from the period of January 1979 till December 2010 and GLDAS-Noah from the periods of January 1979 till December 1995 and of January 1998 till December 2010.



HESSD
9, 11487–11520, 2012

Analysis of long-term terrestrial water storage variations

Y. Huang et al.

Title Page
Abstract | Introduction
Conclusions | References
Tables | Figures
◄ | ►
◄ | ►
Back | Close
Full Screen / Esc
Printer-friendly Version
Interactive Discussion

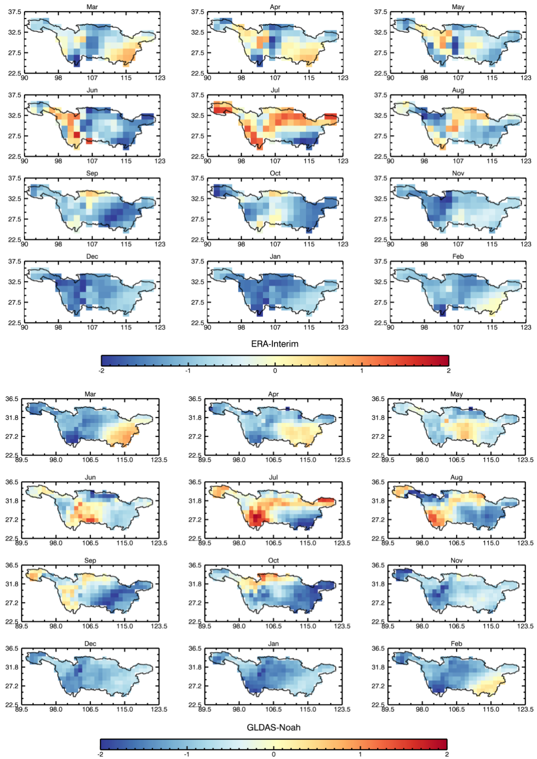


**Fig. 5.** Spatial patterns of monthly averaged TWS annual standardized anomalies from ERA-Interim computed from the period of January 1979 till December 2010 and GLDAS-Noah from the periods of January 1979 till December 1995 and of January 1998 till December 2010.





HESSD

9, 11487–11520, 2012



Title Page
Abstract | Introduction
Conclusions | References
Tables | Figures
◀| |▶
◀ ▶
Back | Close
Full Screen / Esc
Printer-friendly Version
Interactive Discussion

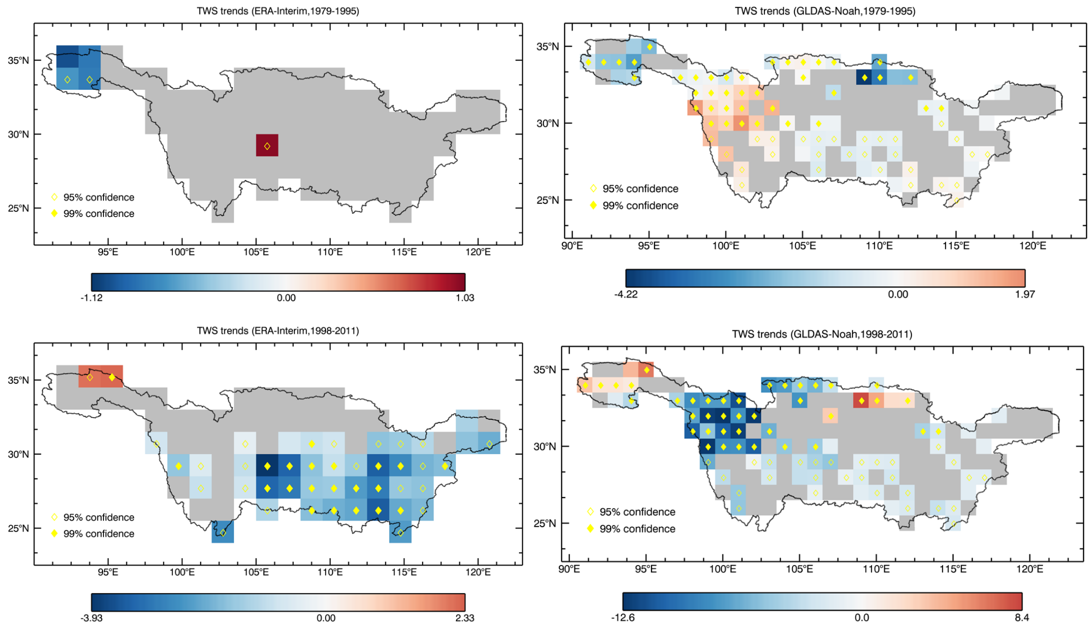


**Fig. 6.** ERA-Interim estimated and GLDAS-Noah estimated TWS annual trends between 1979–1995 and between 1998–2010 in millimeters per year (gray grids represent insignificant trends; the cell with an empty diamond indicates the trend passes the 95 % confidence level; the cell with a filled diamond indicates the trend passes the 99 % confidence level; others indicate the trends passes the 90 % confidence level).

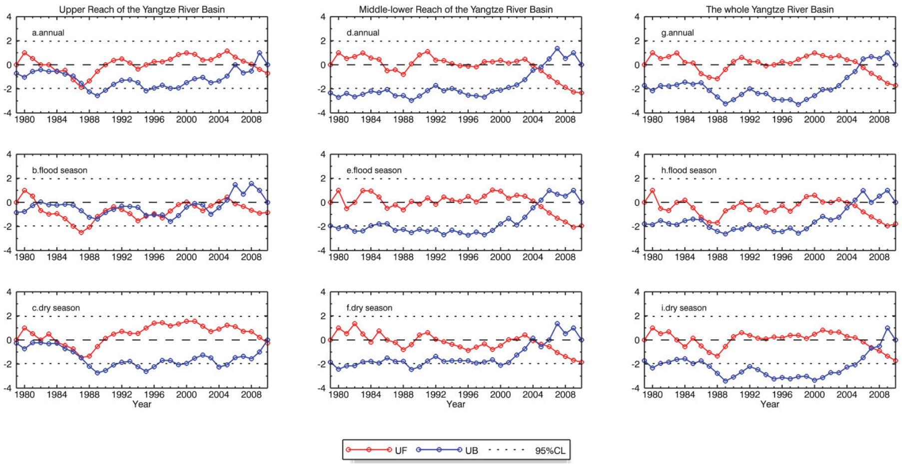


**Fig. 7.** The forward (UF) and backward (UB) Mann-Kendall statistic rank series for TWS standardized anomalies of annual **(a, d, g)**, flood season **(b, e, h)** and dry season **(c, f, i)** during the period between 1979 and 2010 in upper reach, middle-lower reach and the whole Yangtze River basin, respectively (the horizontal dotted lines represent the critical values corresponding to the 95 % confidence level).





HESSD
9, 11487–11520, 2012

Analysis of long-term terrestrial water storage variations

Y. Huang et al.

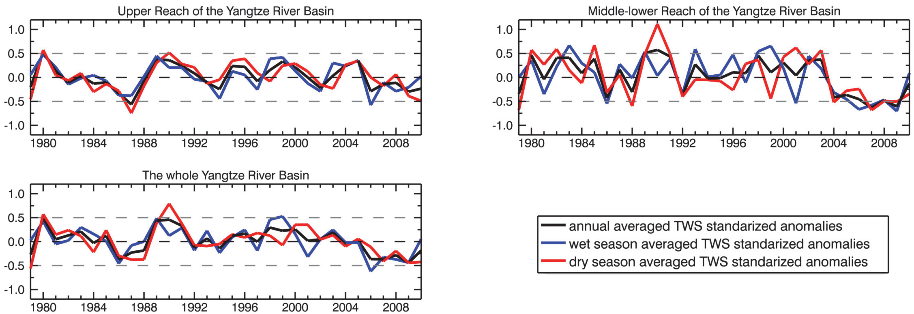


**Fig. 8.** The time series of the annual, wet season (May–October) and dry season averaged (November–April) TWS standardized anomalies in the upper, middle-lower Yangtze reach and the whole Yangtze River basin, respectively.





HESSD
9, 11487–11520, 2012